

Transcript signature predicts tissue NK cell content and defines renal cell carcinoma subgroups independent of TNM staging

Judith Eckl · Alexander Buchner · Petra U. Prinz ·
Rainer Riesenberg · Sabine I. Siegert ·
Robert Kammerer · Peter J. Nelson · Elfriede Noessner

Received: 2 May 2011 / Revised: 4 July 2011 / Accepted: 11 August 2011 / Published online: 26 August 2011
© Springer-Verlag 2011

Abstract Clear cell renal cell carcinoma (ccRCC) is an aggressive and difficult to manage cancer. Immunotherapy has the potential to induce long-lasting regression in a small group of patients. However, severe side effects limit broad application which highlights the need for a marker to distinguish responder from nonresponder. TNMG staging, referring to tumor size, lymph node involvement, presence of metastasis, and grade of tumor differentiation, represents an important prognostic system but is not useful for predicting responders to immunotherapy. NK cells are potent antitumor effector cells, and a role as prognostic marker in some solid tumors has

been suggested. As NK cells are responsive to various immune modifiers, they may be important mediators of patient response to immunotherapies, in particular those including IL-2. We report that the NK cell percentage within RCC-infiltrating lymphocytes, as determined by flow cytometry, allows ccRCC subgrouping in NK^{high}/NK^{low} tissues independent of TNMG classification. Quantitative reverse transcriptase polymerase chain reaction using whole-tissue RNA identified four markers (NKp46, perforin, CX₃CL1, and CX₃CR1) whose transcript levels reproduced the NK^{high}/NK^{low} tissue distinction identified by flow cytometry

JE and AB share first authorship, and EN and PJN share senior authorship.

Electronic supplementary material The online version of this article (doi:10.1007/s00109-011-0806-7) contains supplementary material, which is available to authorized users.

J. Eckl
Clinical Cooperation Group “Immune Monitoring”,
Institute of Molecular Immunology, Helmholtz Zentrum
München—German Research Center for Environmental Health,
Marchioninistrasse 25,
81377 Munich, Germany

A. Buchner · R. Riesenberg
Tumor Immunology Laboratory, LIFE Center,
Marchioninistrasse 23,
81377 Munich, Germany

A. Buchner
Department of Urology, University Clinic Grosshadern,
Marchioninistrasse 15,
81377 Munich, Germany

S. I. Siegert
Institute of Pathology, Ludwig-Maximilians-University,
Marchioninistrasse 27,
81377 Munich, Germany

R. Kammerer
Institute of Immunology, Friedrich-Loeffler-Institut,
Paul-Ehrlich-Strasse 28,
72001 Tübingen, Germany

P. J. Nelson
Clinical Biochemistry, Medical Policlinic,
Ludwig Maximilians University Munich,
Schillerstrasse 42,
80336 Munich, Germany

P. U. Prinz · E. Noessner (✉)
Institute of Molecular Immunology, Helmholtz Zentrum
München—German Research Center for Environmental Health,
Marchioninistrasse 25,
81377 Munich, Germany
e-mail: noessner@helmholtz-muenchen.de

with high selectivity and specificity. Combined in a multiplex profile and analyzed using neural network, the accuracy of predicting the NK^{high}/NK^{low} groups was 87.8%, surpassing that of each single marker. The tissue transcript signature, based on a robust high-throughput methodology, is easily amenable to archive material and clinical translation. This now allows the analysis of large patient cohorts to substantiate a role of NK cells in cancer progression or response to immunotherapy.

Keywords NK cells · Transcript signature · Renal cell carcinoma · Prognosis · Immunotherapy

Introduction

Renal cell carcinoma (RCC) is the most common type of kidney cancer and follows an unpredictable disease course [1]. The TNMG staging system, which defines local extension of the primary tumor (T), involvement of regional lymph nodes (N), the presence of distant metastasis (M), and the tumor cell grade of differentiation (G), is currently the most applied prognostic approach, but accurate estimation of prognosis remains imprecise [2]. Current efforts are directed toward the identification of new markers that would improve prediction of prognosis (prognostic markers) and help stratify patients for treatment strategies (predictive markers). Targeted therapies have improved the management of metastatic disease [3], but immunotherapy, in particular high-dose IL-2, remains the only treatment that can induce cure in a subgroup of patients with metastatic RCC [4]. It is not understood why some patients are responders, whereas others exhibit tumor progression under identical therapies. RCC tissues are densely infiltrated with immune effector cells (references in [5]), but it is unclear how the infiltrate relates to tumor growth control (prognosis) or to the patient's responsiveness to therapy (prediction).

NK cells are cytotoxic effector cells that can kill tumor cells. They are powerful antileukemia effector cells [6], and a role in some solid tumors has been suggested [7–9]. Partial regression of primary tumor growth in melanoma patients has been correlated with NK cell activity in some patients suggesting that NK cells may represent a potential prognostic marker [10, 11]. However, studies directed toward this issue have been hampered by technical limitations of NK cell quantification in tissues.

We previously reported that clear cell (cc)RCC tumors can be subdivided based on a high (NK^{high}) or a low percentage (NK^{low}) of NK cells present in the tumor-infiltrating lymphocytes (TILs, cutoff: 20% NK within TILs) [12]. Based on the observation that NK cells from NK^{high} tumors responded to ex vivo IL-2 treatment with gain of cytolytic

activity, it is possible that a high NK cell content in RCC tumors may help predict response to IL-2 therapy.

The current procedure for the discrimination of NK^{high} from NK^{low} tumors requires fresh postsurgery tissue for flow cytometry of isolated tumor-infiltrating leukocytes and thus is not compatible with the analysis of archive tissues from large retrospective studies or to monitor prospective trails. A reliable molecular tissue profile that would reproduce the FACS-based (FC) quantification of NK cell infiltration in the tissue would allow the analysis of large archive cohorts and, thus, could be applied to refine and expand our understanding of an NK cell contribution to disease processes or response to immunotherapy.

We here report that subgrouping of ccRCC tissues according to the percentage of NK cells among TILs is independent of the TNMG classification and could be a prognostic marker for ccRCC disease outcome. Using whole-tissue RNA isolated from ccRCC tissues and applying quantitative reverse transcriptase polymerase chain reaction (RT-qPCR), specific gene transcripts were identified that reproduced the FC-NK^{high}/NK^{low} discrimination of tumors with high selectivity and specificity. Highest accuracy was achieved when the markers were combined in a multiplex profile and analyzed using neural network. The tissue transcript signature, determined by a robust high-throughput RT-qPCR methodology, is easily amenable to archive material allowing the analysis of large patient cohorts. This will help substantiate a role of NK cells as prognostic factor for disease outcome or as predictive marker for response to immunotherapy. Moreover, the transcript signature may be used in other disease pathologies, where an involvement of NK cells is suspected.

Material and methods

RCC tissues and patient information

RCC tissues were obtained from untreated patients [Departments of Urology, Ludwig-Maximilians-University (LMU); Urological Clinic Planegg, Munich, Germany] and were histopathologically evaluated as ccRCCs (Department of Pathology, LMU, Munich). Samples were snap-frozen within 30 min of nephrectomy and stored at -86°C. The sample collection was done with the approval of the local ethics committee (Ethikkommission der Medizinischen Fakultät der LMU) with written informed consent of the probands. Patient characteristics are listed in Table 1 (updated from [12]). None of the patients had received any therapy before surgery as there are no neoadjuvant (presurgery) therapies for RCC [3]. Thus, the NK cell content as well as the transcript profile were established from therapy-naïve tumors. Metastatic patients may receive systemic adjuvant therapy [3, 4]. In

Table 1 Patient demographics and tumor characteristics

Patient ID	Sex	Age ^a	T N M G ^b	Follow-up ^c	NK in TILs (FACS) ^d	NK in TILs (ANN) ^e
1	m	67	T1b N0 M0 G2	A (53)	High	High
2	f	31	T2 N0 M0 G2	A (40)	High	High
3	f	61	T1a N0 M0 G2	A (66)	High	High
4	f	66	T1b N0 M0 G2	A (43)	High	High
5	m	52	T1 N0 M0 G3	A (62)	High	Low
6	m	47	T2 N0 M0 Gx	A (39)	High	High
7	m	68	T3b N0 M0 G2	A (93)	High	High
8	m	68	T3b N0 M0 G2	DOD (34)	High	Low
9	f	76	T3b N0 M0 G2	A (66)	High	Low
10	f	67	T3b N0 M0 G2	A (67)	High	High
11	f	74	T3a Nx M0 G3	n.d.	High	High
12	m	59	T3b Nx M0 G2	A (37)	High	High
13	m	77	T3 Nx M1 G2	D* (12)	High	High
14	m	49	T2 N0 M0 G2	n.d.	High	High
15	m	53	T3b N0 M0 G2	n.d.	High	High
16	m	50	T2 Nx M0 G2	n.d.	High	High
17	m	34	T2 N0 M0 G2	PR (63)	Low	Low
18	m	47	T1b N0 M0 G2	DOD (35)	Low	Low
19	m	57	T2 N0 M0 G3	A (62)	Low	Low
20	f	69	T1 Nx M0 G2	A (42)	Low	Low
21	m	68	T1 N0 Mx G2	A (67)	Low	Low
22	m	83	T2 N0 M0 G2	A (139)	Low	Low
23	m	61	T3 N0 M0 G3	D" (38)	Low	High
24	m	74	T3b N0 M1 G3	DOD (55)	Low	Low
25	m	53	T3b N0 M0 G2	A (17)	Low	Low
26	f	74	T3b N0 M0 G2	D" (36)	Low	Low
27	f	80	T3b N2 M0 G2	DOD (76)	Low	Low
28	m	61	T3b N2 M1 G3	DOD (12)	Low	Low
29	f	35	T4 N0 M0 Gx	DOD (51)	Low	Low
30	m	73	T3c N0 M1 G2	DOD (27)	Low	Low
31	m	68	T3b N0 M1 G2	DOD (48)	Low	Low
32	f	80	T1 N0 M1 G3	PR (83)	Low	Low
33	m	67	T3b N0 M0 G2	A (40)	Low	Low
34	m	67	T3b N0 M0 G3	n.d.	Low	High
35	m	58	T3b N0 M0 G2	n.d.	Low	Low
36	f	65	T3b N2 M0 G3	n.d.	Low	Low
37	m	60	T3 Nx M0 G3	PR (16)	Low	Low
38	m	49	T2 N0 M0 G2	n.d.	Low	Low
39	f	57	T2 Nx M1 G3	DOD (3)	Low	Low
40	f	72	T3b N0 M0 G3	DOD (12)	Low	Low
41	f	67	T3b N0 M1 G2	n.d.	Low	Low

Only clear cell RCC were included. None of the patients had received treatment prior to surgery. For clinical data, see “Material and methods” section *m* male, *f* female, *A* alive, *PR* progress, *DOD* dead of disease, *D** dead of unrelated cause, *D"* dead of unknown cause, *n.d.* no follow-up available

^a Age in years at surgery; mean 60.3 years for NK^{high} group and 63.2 for NK^{low} group

^b Postoperative tumor classification according to UICC [1], with T referring to tumor size, N to nodal status, M to the presence of distant metastasis, and G to the tumor differentiation

^c Follow-up was completed until August 2010 with a median follow-up of 45 months (range 3–139 months). Numbers in brackets are months of survival after surgery

^d High/low refers to tissue with either >20% (high) or ≤20% (low) of NK cells among TILs as determined by FACS

^e High/low refers to tissue classified by ANN analysis to express a high or low transcript signature

our patient cohort, 10 patients had metastatic disease (M+ or/ and N+). Five received experimental immunotherapy (anti-G250 antibody, inhalative IL-2, or tumor cell vaccination). Four of the treated patients had progressive disease during/after therapy (cases 28, 30, 31, and 39) and died of RCC, one patient died of unrelated cause (case 13). The remaining patients with metastatic disease did not receive any systemic treatment.

Isolation of tumor-infiltrating leukocytes and NK cell quantification using flow cytometry

Tumor-infiltrating leukocytes were isolated from fresh tumor tissues by mechanical and enzymatic tissue dissociation [12]. NK cells among the tumor-infiltrating lymphocytes were quantified using multicolor flow cytometry. Briefly, $3\text{--}5 \times 10^5$ tumor-infiltrating leukocytes were stained in FACS buffer (PBS, 2% FCS, 2 mmol/L EDTA, 0.1% NaN_3) for 20 min at 4°C with a cocktail of antibodies, anti-CD45-PE-Cy7 (BD Bioscience, Heidelberg, Germany), anti-CD14-APC-Alexa750 (Invitrogen, Darmstadt, Germany), anti-CD19-APC-Alexa780 (eBioscience, Frankfurt, Germany), anti-CD3-PacificBlue (BD), anti-CD56-APC (Beckmann Coulter, Krefeld, Germany), and 7-AAD (Sigma-Aldrich, Krefeld, Germany). Cells were then fixed with 1% paraformaldehyde for 20 min at 4°C. Data acquisition and analysis were done with LSRII (BD) and FlowJo (Tree Star, Inc., Ashland, USA). The lymphocyte population (TIL) within tumor-infiltrating leukocytes was selected based on FSC/SSC characteristics using parallel stained PBMC of healthy individuals as a guideline. Selection of lymphocytes was followed by exclusion of 7-AAD⁺ (dead) cells and duplets. Then, CD45-expressing cells were selected and CD14⁺ myeloid cells excluded. NK cells were identified as CD3⁻CD56⁺ cells within the gated live CD45⁺ CD14⁻ lymphocytes. The percentage of CD3⁻CD56⁺ (NK) cells among the gated lymphocyte population (CD45⁺, CD14⁻, 7-AAD⁻ lymphocytes) represents the frequency of NK cells (supplementary Fig. S1). The combination of antibodies detailed above additionally included anti-NKp46-PE (BD) or anti-CX₃CR1-PE (BioLegend, San Diego) to determine the expression of NKp46 and CX₃CR1 within the gated NK cell population (supplemental Fig. S1c, d).

RNA isolation and quantitative RT-PCR

Total mRNA was isolated from cryoconserved ccRCC tissues (10–20 10- μm tissue cryosections; $n=41$ patients remained for analysis after exclusion of five tissues with poor RNA quality or poor RT-qPCR performance, see below) using Qiagen RNeasy Mini Kit (Qiagen; Duesseldorf, Germany). RNA yield was determined with Qubit-iT RNA Assay Kit

(Invitrogen). One microgram RNA was transcribed into cDNA with random hexamer primers (Roche Diagnostic; Mannheim, Germany) using reverse transcriptase Super Script II (Invitrogen). cDNAs were amplified by RT-qPCR with the Taqman[®] ABI 7700 Sequence Detection System (Applied Biosystems; Weiterstadt, Germany) using commercially available predeveloped Taqman[®] reagents with optimized primer and probe concentrations for CD2, CD56, NKp46, granzyme B, perforin, CXCL10, CXCL12, CX₃CL1, CX₃CR1, and 18SrRNA (Applied Biosystems). Cycle conditions were as follows: after an initial hold of 2 min at 50°C and 10 min at 95°C, the samples were cycled 40 times at 95°C for 15 s and at 60°C for 60 s. Controls, consisting of master mixes without cDNA template, were negative in all runs. The primers and probes were cDNA specific except for 18SrRNA, CX₃CL1, and CX₃CR1. Comparing RT-negative samples with RT-positive samples revealed $\Delta\text{Ct}>6$, indicating that contaminations with genomic DNA were negligible (below 0.6%). All PCR reactions were performed in duplicates. The relative concentration of target gene was determined by the comparative Ct method by subtracting the Ct of the target gene from the Ct of the control gene [13]. Five tissues were excluded from further analysis due to poor RNA quality or ΔCt of the duplicates more than 0.5, leaving data of 41 ccRCC tissues from individual patients for analysis. Samples with a mean Ct of the duplicate of 39 and more cycles were named “under detection limit” for the respective probe. In total, these were three samples (one NK^{high}, two NK^{low}) of the granzyme B probe. 18SrRNA and CD2 were identified as suitable normalization genes using NormFinder algorithm (Multid; GenEx, Göteborg, Sweden). CD2 was used for normalization of markers that are predominantly lymphocyte expressed and, additionally, to mimic the gating process used in the FACS (FC)-based NK cell tissue classification. The concept to use lymphocyte-associated transcript levels for normalization has been described [14]. RT-qPCR values of markers (here the chemokines), expressed by diverse cell types including tumor cells, lymphocytes, and myeloid cells, were normalized to 18SrRNA.

Statistical analysis

Normality testing was performed using Kolmogorov–Smirnov, D’Agostino, Pearson omnibus, and Shapiro–Wilk tests. As they failed to determine normal distribution of the data, statistical tests for nonparametric data were applied. For statistical analysis, the measurements with PCR product under detection limit were given the arbitrary value of 10^{-10} , which was below the lowest value observed for any positive marker in any tissue. Mann–Whitney *U* test and Bonferroni’s correction were used to determine the significance between

the association of marker transcript (Tc) levels and the FC-NK^{high} and NK^{low} tumor subgroups in the dichotomized models. In addition, the association between FC-NK content and marker Tc levels as continuous variables was analyzed by Spearman rank correlation. Receiver operating characteristic (ROC) analysis was employed to assess the performance of marker Tc levels to predict the FC-NK^{high}/NK^{low} subgrouping of ccRCC. The strength of the association is seen by the area under curve (AUC) with values below 0.6 are not considered biologically useful [15]. ROC cutoffs were defined such that best values for the percent of specificity and sensitivity (with a 95% confidence interval) for the prediction of FC-NK^{high} tissues were achieved. The validity of the cutoff point of each Tc level for the prediction of the FC-NK^{high}/NK^{low} tissue group was tested using contingency measurements (Fisher's exact test). Contingency measurement (Fisher's exact test) was also performed to test the associations of Tc levels of individual markers or the FC-NK^{high}/NK^{low} tissue distinction with clinicopathologic data, whereby the dichotomized values of the Tc levels (according to ROC cutoff) were set in relation to dichotomized TNMG parameters (pT1–2 vs T3–4, pN0 vs N+, M0 vs M+, G1–2 vs G3–4). To evaluate whether the combination of marker Tc levels would improve the prediction of FC-NK^{high}/NK^{low} tumors, the Tc levels of markers showing the best association in univariate ROC and contingency analyses were combined in multivariate models using logistic regression and artificial neural network models (ANN) [16]. The BFGS (Broyden–Fletcher–Goldfarb–Shanno) training algorithm was used for ANN training until the error function (sum of squares) reached a minimum. In all cases, the network architecture was a three-layer multilayer perceptron with one hidden layer of neurons. A sigmoid activation function was employed to determine the values to be summed from the four input variables. The final weighting was approximately equal for the four input variables and consistent across the top neural networks. Tc levels were log transformed prior to multivariate regression and ANN analyses.

The association of NK^{high}/NK^{low} ccRCC groups defined by individual Tc levels or the ANN Tc profile with cancer-specific survival was evaluated univariately (Mantel–Cox) and plotted as Kaplan–Meier curves. Follow-up data were available of 32 patients. Two patients had died of undetermined cause, leaving 30 patients for cancer-specific survival analysis. The association between ccRCC groups defined by FC-NK cell percentages and cancer-specific survival was also analyzed by Cox regression models, univariately and after adjusting for primary tumor TNMG stage. All univariate data analyses were performed using GraphPad Prism version 5.01 for Windows (GraphPad Software; San Diego, USA). Multivariate analysis (ANN,

logistic regression, and Cox regression) used STATISTICA 9 (StatSoft Inc.; Tulsa, USA).

Results

NK cell percentage among lymphocytes infiltrating ccRCC tumors identifies ccRCC subgroups independent of the TNMG classification

We previously reported that ccRCC tumors could be divided into two groups based on their percentage of NK cells present in the TILs [12]. The cutoff value for NK^{high} tumors (>20% of NK cells in TILs) was thresholded to the value of NK cell percentages observed in PBLs of healthy donors, which are generally below 15% [17]. Having extended our initial patient panel ($n=41$) and updating patient follow-up data (median 45, range 3–139 months; Table 1), we now report evidence that patients, who have tumors with high NK cell content, have a longer cancer-specific survival (Fig. 1a; Cox–Mantel $p=0.043$). Adjusting for primary tumor stage, lymph node involvement, distant metastasis, or tumor grade, the association was no longer significant (Table S1; p adjusted for T=0.063; p values between 0.144 and 0.195 after adjustment for N, M, or G), indicating that the NK cell percentage among TILs may not be independent of the TNMG classification when considering survival as the analysis endpoint. The proportion of patients having received postsurgery treatment was lower in the NK^{high} group than in the NK^{low} group (one NK^{high} patient, four NK^{low} patients; see “Material and methods” section). Nevertheless, the survival probability of the NK^{high} group was better. Thus, the better survival of the NK^{high} group was not caused by a higher number of treated patients. In the NK^{low} group, which had poorer survival, more patients had received treatment. If treatment would have prolonged life, this would decrease the difference between the groups. Thus, considering a potential bias of treatment may improve the significance of the analysis.

Notably, using Fisher's exact analysis, there was no significant association between the FC-NK^{high}/NK^{low} tissue grouping and the TNMG classification (p values between 0.079 and 0.537, Table 2). Thus, the NK cell percentage of an RCC tissue was not a surrogate of the TNMG classification but could be regarded as a new marker used in addition to the TNMG classification to identify ccRCC subgroups.

Analysis of large patient cohorts will be required to test if the FC-NK^{high}/NK^{low} ccRCC subgrouping has relevance for ccRCC prognosis, in addition to or independent of the TNMG stage and whether it will have value as a new marker independent of TNMG. This is not possible with the current FACS-based NK cell quantification method but

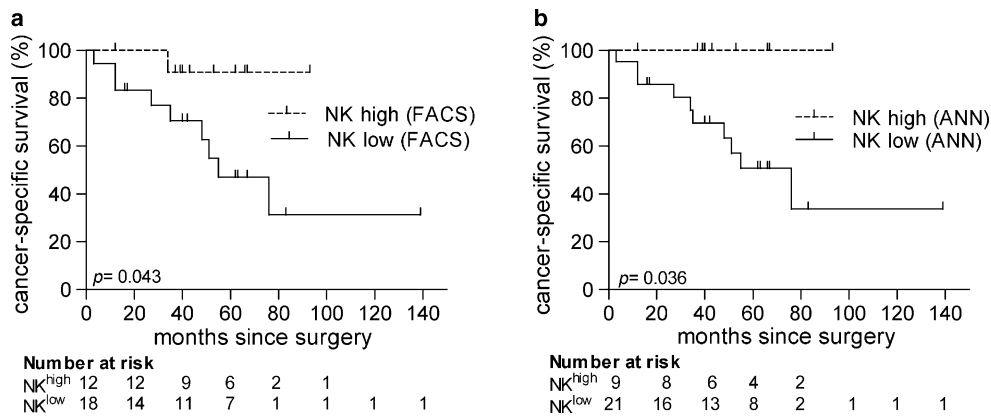


Fig. 1 Univariate association of cancer-specific survival with NK^{high} vs NK^{low} tissue grouping. Thirty ccRCC patients were classified into two groups according to their percentage of NK cells in TILs as determined by FACS (FC) analysis (a) or according to the four-gene transcript signature of artificial neural network (ANN) (b). The

association to cancer-specific survival was analyzed using Kaplan–Meier. p values of the univariate Cox–Mantel test are indicated. Each tick mark represents a censored case. Depicted under the graphs are the number of patients at risk at the given time point. For details on clinical data, see “Material and methods” section

Table 2 Association between NK^{high}/NK^{low} tissue grouping by flow cytometry or transcript levels and TNMG classification using Fisher’s exact test

	p value ^a	PPV	NPV	RR (CI 95%)	LR
FC-NK (% of TIL)					
pT (T1 + T2 vs T3 + T4)	0.518	0.47	0.67	1.4 (0.7–3.0)	1.4
pN (N0 vs N1)	0.537	0.39	1.00		1.3
M (M0 vs M1)	0.114	0.47	0.88	3.8 (0.7–3.0)	1.3
G (G1 + G2 vs G3 + G4)	0.079	0.50	0.83	3.0 (0.8–11.2)	1.5
Tc-NKp46[CD2]					
pT (T1 + T2 vs T3 + T4)	0.756	0.53	0.54	1.2 (0.6–2.2)	1.2
pN (N0 vs N1)	1.000	0.47	0.67	1.4 (0.3–7.3)	1.1
M (M0 vs M1)	0.092	0.56	0.86	3.9 (0.6–24.8)	1.4
G (G1 + G2 vs G3 + G4)	0.506	0.54	0.62	1.4 (0.7–3.0)	1.2
Tc-perforin[CD2]					
pT (T1 + T2 vs T3 + T4)	0.748	0.47	0.62	1.3 (0.6–2.6)	1.3
pN (N0 vs N1)	0.251	0.45	1.00		1.2
M (M0 vs M1)	0.107	0.50	0.88	4.0 (0.6–25.9)	1.4
G (G1 + G2 vs G3 + G4)	0.734	0.41	0.67	1.2 (0.5–3.1)	1.1
Tc-CX ₃ CL1[18SrRNA]					
pT (T1 + T2 vs T3 + T4)	0.759	0.47	0.63	1.3 (0.6–2.6)	1.3
pN (N0 vs N1)	1.000	0.36	0.67	1.1 (0.2–5.7)	1.0
M (M0 vs M1)	0.107	0.50	0.88	4.0 (0.6–25.9)	1.4
G (G1 + G2 vs G3 + G4)	0.076	0.52	0.83	3.1 (0.8–11.6)	1.6
Tc-CX ₃ CR1[CD2]					
pT (T1 + T2 vs T3 + T4)	0.759	0.47	0.58	1.1 (0.6–9.9)	1.1
pN (N0 vs N1)	0.251	0.45	1.00		1.2
M (M0 vs M1)	0.258	0.50	0.75	2.0 (0.6–7.0)	1.2
G (G1 + G2 vs G3 + G4)	0.742	0.48	0.58	1.2 (0.5–2.5)	1.1

The flow cytometry (FC)-based NK cell percentages of TILs of each patient were used as dichotomized variable using the 20% cutoff (Table 1). Transcript (Tc) levels were modeled as dichotomized variable using the cutoff as determined by ROC analysis (Table 3). TNMG variables were modeled as indicated

PPV positive predictive value, NPV negative predictive value, RR relative risk, LR positive likelihood ratio

^a p value (two sided) of the Fisher’s exact test

requires a robust methodology that recapitulates the FACS-based NK^{high}/NK^{low} tissue distinction and is applicable to archival material and large cohorts.

Tissue transcript levels of NKp46, perforin, CX₃CL1, and CX₃CR1 reproduce the ccRCC tissue subgrouping according to FACS-determined high or low NK cell content

Potential markers for NK cell quantification include the activating natural cytotoxicity receptors NKp30, NKp44, and NKp46 that are exclusively expressed on NK cells, CD56, and perforin [7, 18, 19]. An additional class of potential markers includes the chemokine/chemokine receptor family. Chemokine receptors help regulate the leukocyte response and direct their migration to tissues based on the tissue-specific chemokine microenvironment [20, 21].

To identify a molecular tissue signature that reproduces the FC-NK^{high}/NK^{low} discrimination, whole-tissue RNA was prepared from the archived ccRCC tumors where the corresponding fresh tissues had been used for leukocyte isolation and NK cell quantification by flow cytometry ($n=41$; Table 1, updated from [12]). Tc levels of NK- and lymphocyte-associated markers, NKp46, CD56, perforin, granzyme B, CXCL10/IP-10, CXCL12/SDF-1, and CX₃CL1, and the corresponding chemokine receptor (CX₃CR1) were assessed by RT-qPCR and set in relationship to the FC-NK cell frequency among TILs.

Flow cytometry is a lymphocyte-gated strategy yielding percentages of NK cells among TILs rather than absolute numbers of NK cells within the tissue. To reproduce the FACS strategy of NK cell quantification at the transcript level analysis, RT-qPCR data of the lymphocyte-expressed markers, i.e., NKp46, CD56, perforin, granzyme B, and CX₃CR1, were normalized to the common lymphocyte marker CD2, while the chemokines, which are expressed by diverse cell types including tumor cells, lymphocytes, and myeloid cells, were normalized to 18SrRNA.

Tc levels of NKp46 and perforin reproduced the FACS-based NK^{high}/NK^{low} tissue discrimination when normalized to CD2 (p Tc-NKp46[CD2]=0.0002, p Tc-perforin[CD2]=0.02; Fig. 2a), but not when normalized to 18SrRNA (not shown). Tc levels of CD56 and granzyme B did not reproduce the tissue grouping regardless of normalization (Fig. 2a; not shown).

Of the analyzed chemokines (CXCL10, CXCL12, CX₃CL1), the Tc levels of CX₃CL1[18SrRNA] were found to correspond to the FC-NK^{high}/NK^{low} tissue grouping ($p=0.004$, Fig. 2b). Concomitantly, the Tc levels of the corresponding chemokine receptor CX₃CR1 (CD2 normalized) which is expressed on most NK cells of TILs (supplemental Fig. 1d) also distinguished the FC-NK^{high}/NK^{low} tissue subgroups ($p=0.0006$, Fig. 2c). Tc levels of CX₃CR1 normalized to 18SrRNA still segregated the tissues into the NK^{high}/NK^{low} groups, albeit

with lower significance ($p=0.03$; not shown). Uncorrected p values of these associations were interpreted as a measure of strength of evidence for the FC-NK^{high}/NK^{low} discrimination, markers whose Tc levels remained significant after Bonferroni's correction, NKp46[CD2], CX₃CL1[18SrRNA], and CX₃CR1[CD2], were considered robust candidate biomarker for the prediction whether a tissue belonged to the FC-NK^{high} or FC-NK^{low} ccRCC group. Using Spearman correlation, Tc levels of those markers which discriminated the FC-NK^{high}/NK^{low} ccRCC groups as dichotomized variables were found to also correspond to the FC-NK cell percentages as continuous variables (Fig. 2d).

Performance and relevance of marker transcript levels in predicting the FC-based NK^{high}/NK^{low} tumor classification

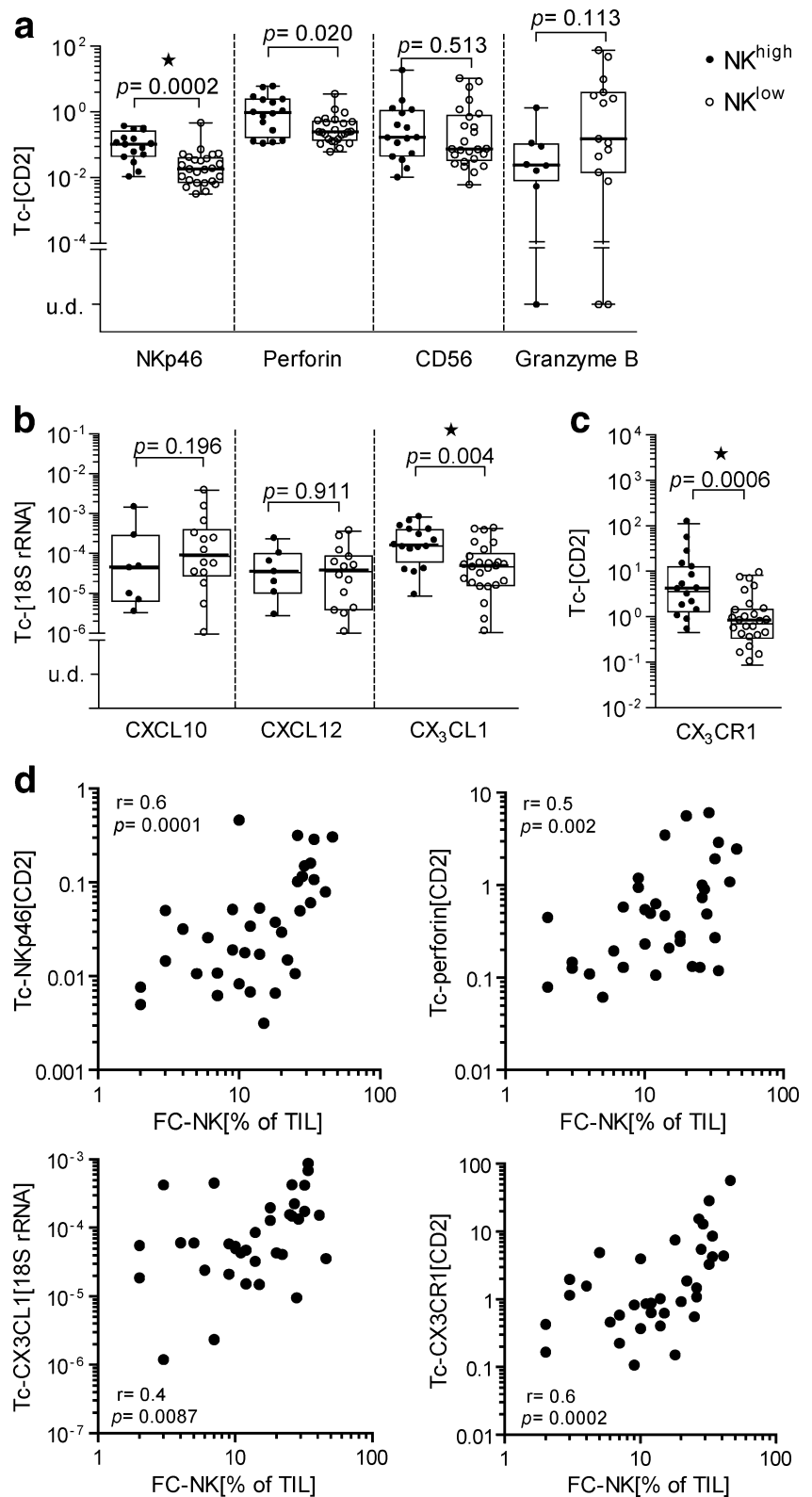
To evaluate the significance of each marker Tc level to distinguish FC-NK^{high} from FC-NK^{low} tumors, ROC analysis was performed for the four discriminating markers (including perforin). AUC and potential cutoff values were calculated and subjected to statistical analysis for specificity and sensitivity using 95% confidence intervals (Table 3). CD2-normalized Tc levels of NKp46, Tc-CX₃CL1 [18SrRNA], and Tc-CX₃CR1[CD2] showed high AUC values and cutoff points separating FC-NK^{high} from FC-NK^{low} tumors with good specificity and sensitivity, providing evidence for a strong overall association of these individual marker Tc levels to the FC-NK^{high}/NK^{low} distinction. The perforin Tc-[CD2] level had the lowest AUC (0.7; 95% CI=0.47–0.85; $p=0.036$) of the four markers and was considered a fair predictor. For comparison, the CD2-normalized Tc level of CD56, which did not correlate with the tissue's FC-NK^{high}/NK^{low} status, had an AUC value below 0.6, which is considered biologically not useful [15].

The validity of the defined cutoffs to predict the FC-NK^{high}/NK^{low} tissue status was tested by Fisher's exact analysis (Table 4). The data revealed good positive and negative predictive values for the Tc levels of all four markers, with Tc levels of perforin again showing the weakest values. Relative risk values of 5.0 for Tc-NKp46 [CD2] and 3.1 for Tc-perforin[CD2] indicated that tissues with values above the ROC cutoff had fivefold and threefold, respectively, higher probability to belong to the FC-NK^{high} group. The overall accuracy of prediction by each individual marker was between 78% (Tc-NKp46 [CD2]) and 73% (Tc-perforin[CD2]) (Table 4).

Transcript levels combined in multivariate analysis improve the prediction of NK^{high} ccRCC tissues

After providing evidence for the independent ability of each marker to predict whether a tissue belonged to the FC-

Fig. 2 Association between tissue transcript levels of select genes and the NK^{high}/NK^{low} ccRCC groups. RNA was isolated from 41 ccRCC tissues with either a high (NK^{high}, $n=16$) or low (NK^{low}, $n=25$) percentage of NK cells among TILs as determined by FACS analysis. Transcript levels of NKp46, perforin, CD56, granzyme B, CXCL10, CXCL12, CX₃CL1, and CX₃CR1 were determined by RT-qPCR. RT-qPCR data of markers expressed by lymphocytes were normalized to CD2 ($Tc-[CD2]$) (a, c). Markers (here the chemokines) (b) that are expressed by many cell types, including tumor cells and thus represent the tissue milieu, were normalized to 18S rRNA ($Tc-[18S\ rRNA]$). Each dot represents the Tc level of one tissue (filled dot NK^{high}, empty dot NK^{low} tissue). *u.d.* refers to tissues where the respective Tc level was under detection limit. *Box plots* indicate the median, the 25th and 75th percentile. Whiskers extend to the lowest and highest value within the group. *p* values were determined by Mann–Whitney *U* test. *p* values are given uncorrected for multiple testing. Indicated by stars are those values which remained significant after correction for multiple comparisons ($p < 0.0064$). **d** Spearman correlation between the FACS-determined NK cell percentages in TILs and the CD2-normalized Tc levels of NKp46, perforin, and CX₃CR1, and the 18S rRNA-normalized Tc levels of CX₃CL1. NK cell percentages as determined by FACS and the transcript values are plotted on a logarithmic scale. Each dot represents one tissue; *R* is the Spearman correlation coefficient and *p* the corresponding *p* value. After adjusting for multiple comparisons, *p* values of < 0.013 were considered significant



NK^{high} or FC-NK^{low} ccRCC group, it was assessed if combining the four markers (NKp46[CD2], perforin[CD2], CX₃CL1[18S rRNA], and CX₃CR1[CD2]) would further

increase the accuracy of prediction. Using the logistic regression model, the accuracy of prediction was 82.9%, thus higher than the accuracy of the best individual marker

Table 3 Receiver operating characteristic (ROC) analysis to assess the performance of transcript levels in predicting NK^{high}/NK^{low} tumors as defined by the NK cell percentage of TILs

RT-qPCR marker (normalization)	<i>p</i> value ^a	AUC (±SEM)	CI 95% ^b	Cutoff ^c	Sensitivity (%)	Specificity (%)
Tc-NKp46[CD2]	0.0004	0.85 (±0.07)	0.63–0.95	0.04	80	82
Tc-perforin[CD2]	0.0360	0.70 (±0.09)	0.47–0.85	0.48	67	68
Tc-CX ₃ CL1[18SrRNA]	0.0080	0.76 (±0.09)	0.59–0.91	0.0001	80	75
Tc-CX ₃ CR1[CD2]	0.0006	0.82 (±0.06)	0.69–0.95	1.70	76	75
Tc-CD56[CD2]	0.5130	0.57 (±0.10)	0.33–0.70	0.14	60	63

ccRCC tumors were divided into NK^{high} or NK^{low} according to the 20% cutoff value of flow cytometry data of TILs (Table 1)

AUC area underneath the curve, SEM standard error of the mean

^a *p* value of ROC analysis

^b 95% confidence interval of the AUC

^c Cutoff value of normalized transcript level that is best fit to discriminate FC-based NK^{high} from NK^{low} tissues

(78% for Tc-NKp46[CD2]). None of the four markers was independent from the other, as expected, since they all are related to the tissue’s NK cell content (Table S2). In addition, ANN analysis was performed. Out of 1,000 trained and validated networks, the best five networks achieved accuracies between 85.4% and 87.8% (Table S3), thus they were all higher than the accuracies of the logistic regression or the single markers. The AUC values of ANN varied between 0.88 and 0.90 (Table S3) and were also higher than those of the univariate analysis, which ranged between 0.70 and 0.85 (Table 3). Combining the four markers into a profile improved the accuracy of correctly classifying the tissues in the NK^{high}/NK^{low} FACS subgroups.

Relationship of transcript levels to clinicopathologic variables and cancer-specific survival

The Tc levels of the four markers showed no statistically significant association to the TNMG staging, similar to the observation for the NK cell percentage in TILs (Table 2). In univariate analysis (Cox–Mantel), patients with a tumor

showing high Tc levels of NKp46[CD2] (*p*=0.029) or a high Tc signature as classified by ANN (*p*=0.036) showed better RCC-specific survival (Fig. 1, Table 5).

Discussion

NK cells are potent innate immune effector cells that can eliminate infected or malignant cells. Increased NK cell content in tissue has been suggested to correlate with better disease prognosis in some solid tumors [7–11]. In addition to cancer, there is wider interest in NK cells in transplant acceptance [22], pregnancy [23] and the regulation of autoimmune disease [24, 25]. In a model of multiple sclerosis, the number of NK cells in the central nervous system was found to correlate to suppression of inflammation and limiting autoimmune pathology [26].

Studies of NK cell frequency and disease prognosis have been hampered in large part due to technical limitations and the lack of a clinically applicable method for the analysis of small amounts of tissues from archival material. Histology

Table 4 Relevance of transcript levels for the prediction of NK^{high}/NK^{low} tissue grouping as determined by flow cytometry using Fisher’s exact test

	<i>p</i> value ^a	PPV	NPV	RR (CI 95%)	LR	Overall accuracy (%)
FC-NK (% of TIL)						
Tc-NKp46[CD2]	0.0005	0.68	0.86	5.0 (1.7–15.0)	3.4	78
Tc-perforin[CD2]	0.086	0.65	0.79	3.1 (1.3–7.3)	2.9	73
Tc-CX ₃ CL1[18SrRNA]	0.0009	0.71	0.83	4.2 (1.6–10.9)	3.8	78
Tc-CX ₃ CR1[CD2]	0.003	0.67	0.83	3.8 (1.5–9.9)	3.1	77

The flow cytometry (FC)-based NK cell percentages of TILs of each patient were used as dichotomized variable using the 20% cutoff (Table 1). Transcript (Tc) levels were modeled as dichotomized variable using the cutoff as determined by ROC (Table 3)

PPV positive predictive value, NPV negative predictive value, RR relative risk, LR positive likelihood ratio

Table 5 Univariate analysis (Cox–Mantel) of an association between cancer-specific survival and patient NK^{high}/NK^{low} grouping according to either FC-based NK cell percentages or the transcript levels

Classification method	Group (number of patients)	<i>p</i> value ^a	Median survival (months)	HR (CI 95%)
FC-NK (% of TILs)	High (12)	0.043	n.a.	0.27 (0.08–0.96)
	Low (18)		55	
NK [ANN]	High (9)	0.036	n.a.	0.23 (0.06–0.91)
	Low (21)		55	
Tc-NKp46[CD2]	High (12)	0.029	84.5	0.25 (0.07–0.87)
	Low (18)		51	
Tc-perforin[CD2]	High (10)	0.351	n.a.	0.52 (0.13–2.05)
	Low (20)		76	
Tc-CX ₃ CL1[18SrRNA]	High (13)	0.097	76	0.35 (0.1–1.21)
	Low (17)		55	
Tc-CX ₃ CR1[CD2]	High (12)	0.225	n.a.	0.45 (0.12–1.63)
	Low (18)		76	

The flow cytometry (FC)-based NK cell percentages of TILs of each patient were used as dichotomized variable using the 20% cutoff (Table 1). Transcript (Tc) levels were modeled as dichotomized variable using the cutoff as determined by ROC (Table 3)

^a *p* value of Mantel–Cox test

n.a. not applicable (median survival has not been reached yet), *HR* hazard ratio

used to quantify NK cells is limited by the lack of individual markers that unambiguously identify NK cells [18, 19]. Single markers such as CD56 have been shown to falsely identify NK cells [27], as CD56 is also expressed by other lymphocytes which are often elevated in tissues [18, 28]. NKp46, a marker unique to NK cells, can also be problematic in histology or FACS analysis as protein levels of NKp46 can be downregulated in some situations [6, 19, 29], including NK cells in TILs of ccRCC (supplemental Fig. 1c). Flow cytometry, which allows marker combinations, is a method of choice for the quantification of cell types that require more than one marker for distinction from other cell types. Identification of NK cells by flow cytometry as CD3[−]CD56⁺ cells has proven reliable, outperforming the utilization of NKp46 due to its downregulation in RCC tumors. However, flow cytometry requires live cell suspensions and thus relies on the availability of sufficient fresh surgical material to isolate the leukocyte infiltrate, which makes its application impossible for biopsy material or archival tissue. The development of a method for NK cell quantification that is easily applicable to diverse tissue sources would improve our understanding of the role of NK cells in disease pathogenesis.

Here we report that transcript levels of NKp46 and perforin, normalized to the lymphocyte-associated CD2 transcript levels, the chemokine CX₃CL1 (normalized to 18SrRNA), and its corresponding NK cell-expressed receptor CX₃CR1 (normalized to CD2) allowed statistically significant prediction of the NK^{high}/NK^{low} tissue classification based on flow cytometry NK cell frequencies among TILs of ccRCC tissues. Neither CD56 nor granzyme B

transcript levels, commonly assumed to be strongly associated with NK cells, showed predictive power. The lack of association was not unexpected based on their expression by other lymphocytes [18, 28]. The predictive value of the Tc levels required the appropriate normalization strategy for the lymphocyte-expressed markers. Tc-NKp46 or Tc-perforin was only able to reproduce the FC-based NK^{high}/NK^{low} tissue grouping when normalized to the common lymphocyte marker CD2, which mimicked the lymphocyte-gated quantification strategy of flow cytometry.

NKp46 and perforin are common NK-associated markers and likely predict the NK cell content independent of the tissue milieu or disease. However, perforin can be downregulated in cancer and chronic viral situations [30, 31] which could explain the observed weak predictive value for ccRCC tissues. The chemokine milieu may show tissue-specific variations. Thus, different ligand/receptor pairs can have predictive value in different tissue types. Tissue-specific differences may explain why transcript levels of CXCL10 and CXCL12 which had been associated with NK cell recruitment in other organ systems [25, 32] had no predictive value in the context of our ccRCC tissues. CX₃CL1 plays an important role as an adhesion molecule, chemotactic factor, and costimulator of cytotoxicity of CX₃CR1⁺ NK cells [33]. An association of NK cells with the CX₃CR1/CX₃CL1 axis has been documented in various tissue settings [33–35]. Thus, a transcript signature based on Tc levels of NKp46, CX₃CL1, CX₃CR1, and potentially perforin should be broadly applicable for NK cell quantification across different tissue types, including cancer, autoimmune disease, viral infections, and disorders of the maternal–fetal tolerance.

Each transcript parameter details a different feature of an NK cell or tissue factor (i.e., chemokines that potentially contribute to NK cell recruitment). Not all markers may concomitantly be present in an individual sample. Therefore, combining the markers into a multiplex profile should best describe the NK cell content in a tissue, possibly explaining why the multiplex analysis surfaced as the most accurate way in predicting the NK cell frequency within the RCC's lymphocyte infiltrate. However, CD2-normalized transcript levels of NKp46 were found to accurately predict the RCC tissue NK cell content and may, therefore, suffice as a single marker in many situations to predict a tissue's NK cell content.

Testing the NK cell content as a potential prognostic marker for patient survival, it was observed that patients with FC-NK^{high} tumors, tumors with high NKp46 Tc levels, or high ANN signature had a higher survival probability. However, this association appeared not to be independent of the TNMG classification system, which is currently the most important prognostic system. Future analyses of a larger patient cohort with detailed consideration of the postsurgery treatment status are required to allow a founded conclusion as to whether a patient's tumor NK cell status contributes to survival prognosis in addition to or independent of the TNMG stage. While this was not possible with the current FACS-based NK cell quantification method, this will now be possible using the transcript analysis.

TNMG, while being the most important prognostic system in RCC, is not useful in predicting responders to immunotherapy. IL-2 therapy has the potential to induce prolonged disease-free survival and even cure in a select subgroup of patients [4]. Yet, this treatment comes with severe life-quality impairing toxicity preventing its broad application. Because there is no marker to predict responders, potentially responding patients may not receive the treatment while others are undergoing treatment and toxicity without being able to derive benefit.

Notably, here we found that the subgrouping according to the FC-based NK cell percentages, the transcript levels, or the ANN profile of NKp46, perforin, CX₃CL1, and CX₃CR1 was independent of TNMG, revealing the NK cell content of the RCC tissue as a potential new marker to identify ccRCC subgroups different from the TNMG stage. NK cells are responsive to IL-2, and as shown in our previous analysis [12], NK cells of the NK^{high} ccRCC group acquired cytotoxicity after in vitro IL-2 treatment. Thus, the frequency of NK cells in the tumor could be of importance for the response to IL-2 therapy. Exploring the value of the RCC tissue NK cell content as a predictive marker for response to immunotherapies, in particular those including IL-2, will now be possible by analyzing retrospectively the transcript signature of tissue collections of patient cohorts who received immunotherapy and were identified as either responders or nonresponders to therapy.

The gene signature may also be useful in the characterization of tissue of other disease pathologies where an involvement of NK cells has been proposed, such as multiple sclerosis, pregnancy, or transplant rejection. In situations where CX₃CL1/CX₃CR1 seems dispensable, single marker analysis of NKp46 Tc levels, with or without perforin, may be considered to estimate the content of NK cells in the tissue.

Acknowledgments We thank A. Brandl, A. Mojaat, and A. Wechselberger for the excellent technical assistance and R. Oberneder (Urology Clinic Dr. Castringius, Munich-Planegg, Germany) for the help with the tissue collection. Financial support for this research was given by grants from the Deutsche Forschungsgemeinschaft, Sonderforschungsbereich Transregio SFB-TR36 (P.J. Nelson, E. Noessner) and Sonderforschungsbereich SFB455 (E. Noessner) and a grant from the European Union EU P6 "INNOCHEM" (P.J. Nelson).

Conflicts of interest The authors declare no conflicts of interest.

References

- Moch H, Artibani W, Delahunt B, Ficarra V, Knuechel R, Montorsi F, Patard JJ, Stief CG, Sulser T, Wild PJ (2009) Reassessing the current UICC/AJCC TNM staging for renal cell carcinoma. *Eur Urol* 56:636–643
- Ficarra V, Galfano A, Mancini M, Martignoni G, Artibani W (2007) TNM staging system for renal-cell carcinoma: current status and future perspectives. *Lancet Oncol* 8:554–558
- Gore ME, Larkin JM (2011) Challenges and opportunities for converting renal cell carcinoma into a chronic disease with targeted therapies. *Br J Cancer* 104:399–406
- Wong MK (2008) The current role of immunotherapy for renal cell carcinoma in the era of targeted therapeutics. *Curr Oncol Rep* 10:259–263
- Frankenberger B, Noessner E, Schendel DJ (2007) Immune suppression in renal cell carcinoma. *Semin Cancer Biol* 17:330–343
- Fauriat C, Just-Landi S, Mallet F, Arnoulet C, Sainty D, Olive D, Costello RT (2007) Deficient expression of NCR in NK cells from acute myeloid leukemia: evolution during leukemia treatment and impact of leukemia cells in NCR^{dull} phenotype induction. *Blood* 109:323–330
- Smyth MJ, Hayakawa Y, Takeda K, Yagita H (2002) New aspects of natural-killer-cell surveillance and therapy of cancer. *Nat Rev Cancer* 2:850–861
- Albertsson PA, Basse PH, Hokland M, Goldfarb RH, Nagelkerke JF, Nannmark U, Kuppen PJ (2003) NK cells and the tumour microenvironment: implications for NK-cell function and anti-tumour activity. *Trends Immunol* 24:603–609
- van Herpen CM, van der Laak JA, de Vries IJ, van Krieken JH, de Wilde PC, Balvers MG, Adema GJ, De Mulder PH (2005) Intratumoral recombinant human interleukin-12 administration in head and neck squamous cell carcinoma patients modifies locoregional lymph node architecture and induces natural killer cell infiltration in the primary tumor. *Clin Cancer Res* 11:1899–1909
- Hersey P, Hobbs A, Edwards A, McCarthy WH, McGovern VJ (1982) Relationship between natural killer cell activity and histological features of lymphocyte infiltration and partial regression of the primary tumor in melanoma patients. *Cancer Res* 42:363–368

11. Imai K, Matsuyama S, Miyake S, Suga K, Nakachi K (2000) Natural cytotoxic activity of peripheral-blood lymphocytes and cancer incidence: an 11-year follow-up study of a general population. *Lancet* 356:1795–1799
12. Schleypen JS, Baur N, Kammerer R, Nelson PJ, Rohrmann K, Grone EF, Hohenfellner M, Haferkamp A, Pohla H, Schendel DJ et al (2006) Cytotoxic markers and frequency predict functional capacity of natural killer cells infiltrating renal cell carcinoma. *Clin Cancer Res* 12:718–725
13. Schmid H, Cohen CD, Henger A, Schlondorff D, Kretzler M (2004) Gene expression analysis in renal biopsies. *Nephrol Dial Transplant* 19:1347–1351
14. Mocellin S, Provenzano M, Rossi CR, Pilati P, Nitti D, Lise M (2003) Use of quantitative real-time PCR to determine immune cell density and cytokine gene profile in the tumor microenvironment. *J Immunol Methods* 280:1–11
15. Taylor JM, Ankerst DP, Andridge RR (2008) Validation of biomarker-based risk prediction models. *Clin Cancer Res* 14:5977–5983
16. Zou J, Han Y, So SS (2008) Overview of artificial neural networks. *Methods Mol Biol* 458:15–23
17. Cooper MA, Fehniger TA, Caligiuri MA (2001) The biology of human natural killer-cell subsets. *Trends Immunol* 22:633–640
18. Walzer T, Jaeger S, Chaix J, Vivier E (2007) Natural killer cells: from CD3(–)NKp46(+) to post-genomics meta-analyses. *Curr Opin Immunol* 19:365–372
19. Caligiuri MA (2008) Human natural killer cells. *Blood* 112:461–469
20. Morris MA, Ley K (2004) Trafficking of natural killer cells. *Curr Mol Med* 4:431–438
21. Mantovani A, Allavena P, Sozzani S, Vecchi A, Locati M, Sica A (2004) Chemokines in the recruitment and shaping of the leukocyte infiltrate of tumors. *Semin Cancer Biol* 14:155–160
22. Beilke JN, Kuhl NR, Van Kaer L, Gill RG (2005) NK cells promote islet allograft tolerance via a perforin-dependent mechanism. *Nat Med* 11:1059–1065
23. Moffett-King A (2002) Natural killer cells and pregnancy. *Nat Rev Immunol* 2:656–663
24. Flodstrom M, Shi FD, Sarvetnick N, Ljunggren HG (2002) The natural killer cell—friend or foe in autoimmune disease? *Scand J Immunol* 55:432–441
25. Ottaviani C, Nasorri F, Bedini C, de Pita O, Girolomoni G, Cavani A (2006) CD56brightCD16(–) NK cells accumulate in psoriatic skin in response to CXCL10 and CCL5 and exacerbate skin inflammation. *Eur J Immunol* 36:118–128
26. Hao J, Liu R, Piao W, Zhou Q, Vollmer TL, Campagnolo DI, Xiang R, La Cava A, Van Kaer L, Shi FD (2010) Central nervous system (CNS)-resident natural killer cells suppress Th17 responses and CNS autoimmune pathology. *J Exp Med* 207:1907–1921
27. Halama N, Braun M, Kahlert C, Spille A, Quack C, Rahbari N, Koch M, Weitz J, Kloor M, Zoernig I et al (2011) Natural killer cells are scarce in colorectal carcinoma tissue despite high levels of chemokines and cytokines. *Clin Cancer Res* 17:678–689
28. Pittet MJ, Speiser DE, Valmori D, Cerottini JC, Romero P (2000) Cutting edge: cytolytic effector function in human circulating CD8+ T cells closely correlates with CD56 surface expression. *J Immunol* 164:1148–1152
29. De Maria A, Fogli M, Costa P, Murdaca G, Puppo F, Mavilio D, Moretta A, Moretta L (2003) The impaired NK cell cytolytic function in viremic HIV-1 infection is associated with a reduced surface expression of natural cytotoxicity receptors (NKp46, NKp30 and NKp44). *Eur J Immunol* 33:2410–2418
30. Lieberman J, Shankar P, Manjunath N, Andersson J (2001) Dressed to kill? A review of why antiviral CD8 T lymphocytes fail to prevent progressive immunodeficiency in HIV-1 infection. *Blood* 98:1667–1677
31. Mortarini R, Piris A, Maurichi A, Molla A, Bersani I, Bono A, Bartoli C, Santinami M, Lombardo C, Ravagnani F et al (2003) Lack of terminally differentiated tumor-specific CD8+ T cells at tumor site in spite of antitumor immunity to self-antigens in human metastatic melanoma. *Cancer Res* 63:2535–2545
32. Hanna J, Wald O, Goldman-Wohl D, Prus D, Markel G, Gazit R, Katz G, Haimov-Kochman R, Fujii N, Yagel S et al (2003) CXCL12 expression by invasive trophoblasts induces the specific migration of CD16⁺ human natural killer cells. *Blood* 102:1569–1577
33. Umehara H, Bloom E, Okazaki T, Domae N, Imai T (2001) Fractalkine and vascular injury. *Trends Immunol* 22:602–607
34. Fong AM, Robinson LA, Steeber DA, Tedder TF, Yoshie O, Imai T, Patel DD (1998) Fractalkine and CX3CR1 mediate a novel mechanism of leukocyte capture, firm adhesion, and activation under physiologic flow. *J Exp Med* 188:1413–1419
35. Guo J, Chen T, Wang B, Zhang M, An H, Guo Z, Yu Y, Qin Z, Cao X (2003) Chemoattraction, adhesion and activation of natural killer cells are involved in the antitumor immune response induced by fractalkine/CX3CL1. *Immunol Lett* 89:1–7